Influence of the initial electronic state on minima of high-order harmonic spectrum radiated from hydrogen molecular ion*

Hui-Fang Cui(崔会芳) and Xiang-Yang Miao(苗向阳)†

College of Physics and Information Engineering, Shanxi Normal University, Linfen 041004, *China*

(Received 9 May 2017; revised manuscript received 12 June 2017; published online 10 September 2017)

We theoretically investigate the high-order harmonic generation of the one-dimensional hydrogen molecular ion at fixed intermediate internuclear distance, driven by a multicycle laser field. Our results show that the initial electronic state of the hydrogen molecular ion affects the modulation of the high-order harmonic spectrum, especially the positions of the minima. Based on the two-state model, the underlying physical mechanism of the minimum is analyzed and discussed. Further analysis shows that the different positions of the minima in the different initial electronic states can be understood via the different interferences of the two phase-adiabatic states at the ionization times.

Keywords: the minima of the high-order harmonic spectrum, interference, phase-adiabatic states

PACS: 33.80.Rv, 42.65.Re, 42.25.Hz **DOI:** 10.1088/1674-1056/26/10/103302

1. Introduction

Recently, high-order harmonic generation (HHG) and its application have continuously been investigated as it can be used to produce attosecond laser pulses, and to probe the structure[1–3] and electronic dynamics[4–6] of atoms and molecules. The mechanism of HHG from atoms is described by the semiclassical three-step model:[7] First, the electron escapes from the core by tunnelling through the Coulomb potential barrier, which is distorted by the intense laser field. Second, the electron is accelerated away from its parent ion by the laser field and obtains additional kinetic energy. Finally, the electron recombines with the parent ion and emits HHG photons. Based on the conventional model of strong-field ionization, the electron will leave the atom with the largest probability at the peaks of the laser field. However, the electron dynamics in molecules is qualitatively different from that in atoms due to the more complicated structures of molecules.[8–14] As the simplest molecule, the hydrogen molecular ion (H_2^+) plays an important role in the theoretical and experimental studies of molecular dynamics in laser field.[15–19] Takemoto and Becker reported the observation of multiple ionization bursts (MIBs) within a half cycle of the laser field when H_2^+ is stretched to intermediate internuclear distance.[8,9] They attributed the MIBs to the ultrafast interwell electron transfer, which is the result of the nonadiabatic electron dynamics.[9] They also explored the nonadiabatic electron dynamics at the time of ionization resulting in the minimum generation in the HHG spectrum.[11,14] However, this viewpoint is different from previous perspectives held by those who attributed the minima to the physical mechanism occurring at the time of recombination.[20–28]

The importance of the electronic structure of the molecule in molecular HHG has been pointed out in the previous theoretical and experimental studies.[29–33] In this study, we first investigate the role of the electronic state in HHG minimum from H_2^+ at intermediate internuclear distance based on the nonadiabatic electron dynamics. We directly solve the one-dimensional (1D) Born–Oppenheimer (BO) time-dependent Schrödinger equation (TDSE) and use the ground state and the first excited state respectively as the initial wave state. We observe different electron local populations and spectral features from the different initial states. With the time-frequency analysis and the classical ionization-recombination map, we make a full quantum analysis of the ionization and recombination process. This analysis gives us direct information about the role of nonadiabatic electron dynamics in HHG minimum and allows us to identify the structure of the molecules from the HHG signal. Atomic units are used throughout this paper unless otherwise stated.

2. Theoretical method

All the calculations were performed for the 1D fixed-nuclei model of H_2^+, which exposed to a linearly polarized laser field, by using the parallel quantum wave-packet computer code LZH-DICP.[34,35] In the dipole approximation and the length gauge, the corresponding time-dependent Schrödinger equation is

$$\mathrm{i}\frac{\partial \psi(z,t)}{\partial t} = \hat{H}(z,t)\psi(z,t). \quad (1)$$

*Project supported by the National Natural Science Foundation of China (Grant No. 11404204) and the Program for the Top Young Academic Leaders of Higher Learning Institutions of Shanxi Province, China.

†Corresponding author. E-mail: sxxymiao@126.com

© 2017 Chinese Physical Society and IOP Publishing Ltd

When we consider the linearly polarized laser field along the molecular axis, the Hamiltonian of this system ($e=\hbar=m=1$) is given by

$$\hat{H}(z,t) = T_{\rm e} + V_{\rm C}(z) + V_{\rm I}(z,t), \tag{2}$$

where

$$T_{\rm e} = -\frac{2m_{\rm p}+1}{4m_{\rm p}}\frac{\partial^2}{\partial z^2}$$

denotes the electronic kinetic-energy operator, $m_{\rm p}$ is the proton mass, and z is the electronic coordinate with respect to the center of mass of the two protons. The soft-core Coulomb potential is expressed as

$$V_{\rm C}(z) = -\frac{1}{\sqrt{(z-R/2)^2+1}} - \frac{1}{\sqrt{(z+R/2)^2+1}}, \tag{3}$$

where R is the internuclear distance of the molecular ion.[36] The external interaction between the laser field and the molecule is given by

$$V_{\rm I}(z,t) = \left(1+\frac{m_{\rm e}}{2m_{\rm p}+m_{\rm e}}\right) zE(t). \tag{4}$$

The electric field of the laser pulse is assumed to have the following form:

$$E(t) = f(t)\cos(\omega_0 t), \tag{5}$$

where ω_0 is the angular frequency and $f(t)$ is the envelope function in the following form:

$$f(t) = \begin{cases} E_0 \sin^2(\pi t/T), & (0 \le t \le T), \\ 0, & (\text{otherwise}), \end{cases} \tag{6}$$

where T is the pulse duration and E_0 is the peak strength.

Equation (1) is solved numerically by using the standard second-order split-operator method,[37,38]

$$\psi(z;t+\delta t) = {\rm e}^{-{\rm i}T\delta t/2} e^{-{\rm i}V\delta t}\, {\rm e}^{-{\rm i}T\delta t/2}\psi(z;t) + O(\delta t^3), \tag{7}$$

where T is the kinetic energy operator as in Eq. (2), and V is the interaction potential taking all the potential energy of the system plus a purely imaginary term to produce an absorbing boundary. In this study, we set $R=7$ a.u. The ground and the first excited state energies of this model are $E_{\rm g}=-0.8227$ a.u. and $E_{\rm u}=-0.80986$ a.u., respectively. The eigenstates $1s\sigma_g$ and $2p\sigma_u$ (denoted as $|g\rangle$ and $|u\rangle$) are almost degenerate and well isolated from the higher-lying excited electronic states. As shown in Fig. 1, the two lowest-lying states have opposite parities and their superpositions form two localized states $|R\rangle = (|g\rangle + |u\rangle)/\sqrt{2}$ and $|L\rangle = (|g\rangle - |u\rangle)/\sqrt{2}$,[39,40] where $|R\rangle$ and $|L\rangle$ represent the electron wavepacket that is localized at the right and left protons, respectively. During the interaction with laser pulse, the $|g\rangle$ and $|u\rangle$ mix and thus the electron density oscillates between the two protons. The time step of the wave function propagation is set to be $\delta t = 0.1$ a.u.

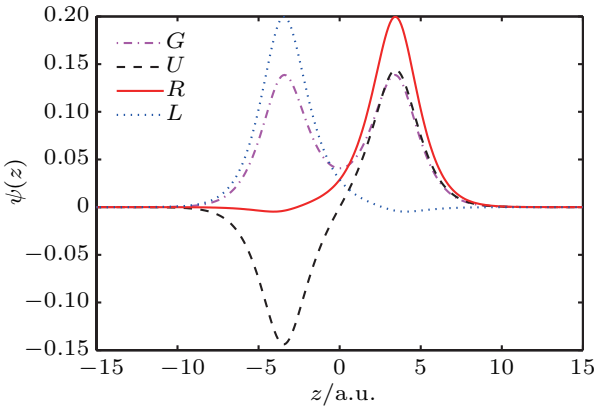


Fig. 1. (color online) Plots of ψ–z of electronic eigenstates $1s\sigma_g$ (G) (mauve dash–dotted line) and $2p\sigma_u$ (U) (black dash line) states, and their superpositions $|R\rangle$ (R) (red solid line) and $|L\rangle$ (L) (blue dotted line).

3. Results and discussion

Figure 2 presents the HHG spectra of H_2^+ initially in its ground state and the first excited state with internucler distance $R=7$ a.u., driven by a 10-cycle full-width infrared laser pulse with wavelength $\lambda = 1400$ nm and peak intensity $I = 1\times10^{14}$ W/cm^2. At first glance, the two spectra show common feature: the plateaus span a broad bandwidth and exhibit almost constant intensity, and then drop steeply at the cutoff. Moreover, considerable suppressions, named interference minima, on the plateau are also observed in both cases. However, we note that the positions of the minima in the two spectra are different.

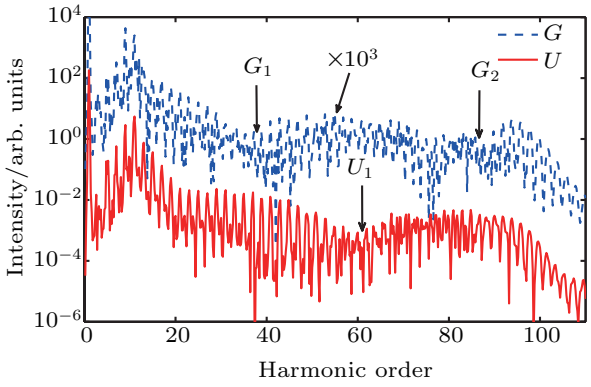


Fig. 2. (color online) High-order harmonic spectra of H_2^+ initially in the ground state (G case) (blue dash line) and in the first excited state (U case) (red solid line) are irradiated by a 1400-nm, 10-cycle, $I_0 = 1\times10^{14}$-W/cm^2 laser pulse. The positions of the spectral minima are marked with black arrows. The harmonic intensitiy of G case is multiplied by factors of 10^3 for the purpose of clarity.

Due to the strong coupling between $|g\rangle$ and $|u\rangle$ in the radiative interaction, we study the underlying mechanisms for the interference minima based on the two-state model. We write the Hamiltonian of the two-state model as[41]

$$H = \begin{pmatrix} E_g & W_{12} \\ W_{21} & E_u \end{pmatrix}, \tag{8}$$

where $W_{12} = \langle g\,|zE(t)|\,u\rangle = W_{21}^*$ is the laser-molecule coupling, E_g and E_u are the eigenvalues of the $|g\rangle$ and $|u\rangle$. The

resulting eigenfunctions are given by

$$|1\rangle = \cos\theta\,|g\rangle - \sin\theta\,|u\rangle,$$
$$|2\rangle = \cos\theta\,|u\rangle + \sin\theta\,|g\rangle, \tag{9}$$

where

$$\theta = \frac{1}{2}\arctan\left[\frac{2\langle g\,|zE(t)|\,u\rangle}{\Delta E_{gu}}\right] \tag{10}$$

with the BO energy separation $\Delta E_{gu} = E_u - E_g$. The eigenvalues are

$$E_{1,2}(t) = \frac{1}{2}\left[E_g + E_u \mp \sqrt{\Delta E_{gu}^2 + 4\,|\langle g\,|zE(t)|\,u\rangle|^2}\right]. \tag{11}$$

The two eigenfunctions $|1\rangle$ and $|2\rangle$ are called "phase-adiabatic" states.

Using the two-phase-adiabatic state model, the total wave function is expressed as

$$|\psi(t)\rangle = \chi_1(t)\,|1\rangle + \chi_2(t)\,|2\rangle, \tag{12}$$

where the time-dependent wave function $\psi(t)$ is obtained from Eq. (7), $\chi_1(t)$ and $\chi_2(t)$ are the time-dependent coefficients associated with $|1\rangle$ and $|2\rangle$.

By projecting the wave function $\psi(t)$ onto the two localized states $|R\rangle$ and $|L\rangle$, we obtain the expressions for the local populations at the respective protons as follows:

$$P_R(t) = \cos^2\left(\theta+\frac{\pi}{4}\right)|\chi_1(t)|^2 + \sin^2\left(\theta+\frac{\pi}{4}\right)|\chi_2(t)|^2 + \mathrm{Re}\left[\cos 2\theta\,\chi_1^*(t)\chi_2(t)\right], \tag{13}$$

$$P_L(t) = \sin^2\left(\theta+\frac{\pi}{4}\right)|\chi_1(t)|^2 + \cos^2\left(\theta+\frac{\pi}{4}\right)|\chi_2(t)|^2 - \mathrm{Re}\left[\cos 2\theta\,\chi_1^*(t)\chi_2(t)\right], \tag{14}$$

where $C(t) = \mathrm{Re}\left[\cos 2\theta\,\chi_1^*(t)\chi_2(t)\right]$ represents the interference between $|1\rangle$ and $|2\rangle$. To examine the validity of the P_R and P_L based on the two phase-adiabatic states model, we calculate the time-dependent populations of the wavepacket localized on the left and right protons as follows:

$$P_R'(t) = \int_0^z |\psi(z;t)|^2\,\mathrm{d}z, \tag{15}$$

$$P_L'(t) = \int_{-z}^0 |\psi(z;t)|^2\,\mathrm{d}z. \tag{16}$$

The time-dependent local populations $P_R(t)$, $P_R'(t)$, and $P_L'(t)$ in the ground state case are presented in Fig. 3(a). From this figure, we note that $P_R'(t)$ and $P_R(t)$ are not equal, which is not unexpected because in the expression of the $P_R(t)$ only the two lowest-lying states $|g\rangle$ and $|u\rangle$ are counted and the higher-lying excited electronic states are not taken into account. Another feature shown from the figure is that the electron motion between the two protons does not always follow the laser-electron interaction. For example, at $t = 819$ a.u. ~ 916 a.u., the oscillating laser electric field $E(t)$ is negative. According to the semi-classical three-step model, the electric field force will push the electron into the $z > 0$ direction and the local population P_R' will gradually increase. Nevertheless,

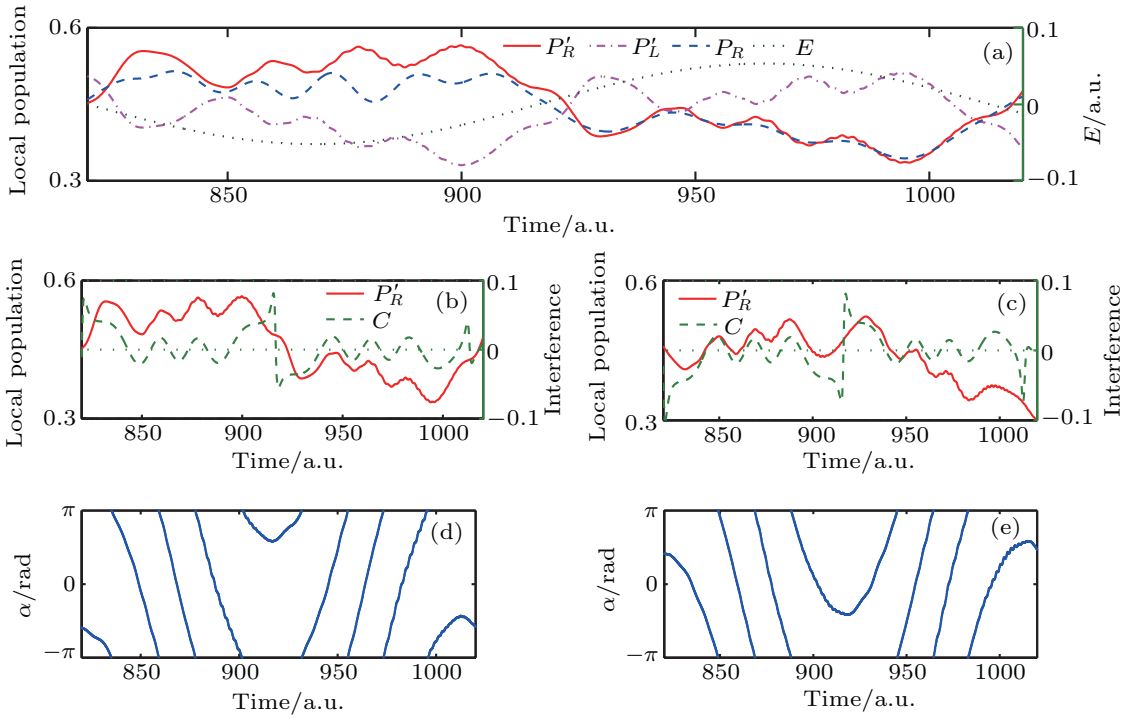


Fig. 3. (color online) (a) Time-dependent local population on the right proton, calculated by two-state model P_R (blue dashed line), by numerical integration P_R' (red solid line) and the local population on the left proton by numerical integration P_L' (mauve dash–dotted line) in the G case. The electric field of the laser pulse is presented in the figure (green dotted line). (b) and (c) Time-dependent local population on the right proton, calculated by numerical integration P_R' (red solid line) and the interference C between the two phase-adiabatic states (green dash line) throughout one laser cycle in the G case and in the U case, respectively. (d) and (e) Evolving relative phase difference between the wave function centered on each proton in the G case and the U case, respectively.

at certain times, we observe P'_R decreasing and P'_L increasing at the same time, which means that at these times the electron transfers from the right well at $z = 3.5$ a.u. to left well at $z = -3.5$ a.u. The interwell electron transfer was reported first in Ref. [41] and they attributed the interwell electron transfer to the interference between the two phase-adiabatic states. He *et al*. also reported this classically forbidden motion of electron in dissociating H_2^+ and named the motion the counter-intuitive motion.[42] Figures 3(b) and 3(c) show the local population $P'_R(t)$ and the interference $C(t)$ between the two phase-adiabatic states in the ground state case (G case) and in the first excited state case (U case), respectively. We find that the counter-intuitive motions of electron keep in step with the interference term in both cases, but these motions occur at different instants. According to the two-state model, we can deduce that the interference term depends not only on the electric field but also on the initial state. Different initial states lead to different coefficients $\chi_1(t)$ and $\chi_2(t)$. Therefore, we attribute the different counter-intuitive motions of electron to the different interferences between the two phase-adiabatic states for the present parameters. References [9] and [14] have reported that the counter-intuitive motions of electron are closely related to the evolving phase difference $\alpha(t) = \arg[\psi(-R_0/2;t)] - \arg[\psi(R_0/2;t)]$. The value of the phase difference α ranges from $-\pi$ to π. In Figs. 3(d) and 3(e), the time-dependent phase difference $\alpha(t)$'s in the G case and U case are presented. By comparing the phase differences (Figs. 3(d) and 3(e)) with the local populations (Figs. 3(b) and 3(c)), we note that the counter-intuitive motion of the electron occurs when the phase difference passes through $-\pi$ (or π), and at moment when the electron is most located on the counter-intuitive side of the molecule, $\alpha = 0$. Compared with the events in the G case, the counter-intuitive events occur at different moments in the U case. This is maybe the reason why the positions of the minima are different in the two cases.

In order to verify the viewpoint, we perform the time-frequency analysis by means of the wavelet transform,[40]

$$d_\omega(t) = \int a(t')\sqrt{\omega_0}W\left(\omega_0\left(t'-t\right)\right)\mathrm{d}t', \tag{17}$$

where $W(x) = \left(1/\sqrt{\tau}\right)\mathrm{e}^{\mathrm{i}x}\mathrm{e}^{-x^2/2\tau^2}$ is the complex Morlet wavelet and $a(t)$ is the time-dependent dipole acceleration of the electron. Figures 4(a) and 4(b) show the time-frequency distributions corresponding to the G case and U case, respectively. We focus on the ionization times between 819 a.u. and 916 a.u. In the G case, in each half cycle, there are two suppressed harmonic emissions denoted as G_1 and G_2 on the short quantum path, which match the spectral positions of the minima presented in Fig. 2. There is also one suppressed harmonic emission labeled G_3 on the long quantum path. However, the corresponding harmonics of G_3 are not obviously linked to the spectrum minimum because the intensity of the long quantum path is much weaker than the short quantum path in this harmonic region, which can be seen from Fig. 4(a). In the U case, there are two obvious suppressed harmonic emissions denoted as U_1 and U_2 in each half cycle, but only the suppressed harmonic emission U_1 contributes predominantly to HHG minimum and the suppressed harmonic emission denoted as U_2 is not observed in the spectrum due to the same reason as the case of G_3. In order to in depth understand the mechanism of the suppressed harmonic emission, we investigate the classical electron dynamics by solving Newton's equation of motion for an electron in the laser field described in Eq. (5). The electron is assumed to be a negative point charge, and is released from one of the protons of the molecule with $\dot{z} = 0$ throughout the ionization interval. Assuming that the recombination happens at the instances when $z = R/2$ or $z = -R/2$, each classical trajectory links a unique pair of ionization and recombination times [cf. Fig. 4(c)]. For the H_2^+, there are four ionization-recombination channels in molecular HHG, i.e., $\mathrm{H}(-) \to e \to \mathrm{H}(+)$, $\mathrm{H}(-) \to e \to \mathrm{H}(-)$, $\mathrm{H}(+) \to e \to \mathrm{H}(-)$, and $\mathrm{H}(+) \to e \to \mathrm{H}(+)$, where $\mathrm{H}(-)$ represents the proton located at $z = -3.5$ and $\mathrm{H}(+)$ represents the proton located at $z = 3.5$. The ionization and recombination times of the four channels are presented in Fig. 4(c). To characterize the interference dynamics, figures 4(d) and 4(e) present the variations of the phase difference α at the time of ionization in the G case and in the U case, respectively. In the G case, during the ionization times of 819 a.u.–916 a.u., there are three instants at which $\alpha = 0$ denoted as G'_1, G'_2, and G'_3 shown in Fig. 4(d). As shown in Fig. 4(c), the electron ionized from $\mathrm{H}(-)$ around 849 a.u. (G'_1) is accelerated by the $E < 0$ field, and then recombines with $\mathrm{H}(+)$ and emits the 39th–40th harmonics around 856 a.u.–866 a.u. (G_1) which corresponds to the suppressed harmonic emission G_1 in Fig. 4(a). The electron ionized from $\mathrm{H}(+)$ around 887 a.u. (G'_2) recombines with $\mathrm{H}(-)$ and emits the 80th–85th harmonics around 983 a.u. (G_2) and this position is consistent with the suppressed harmonic emission G_2 shown in Fig. 4(a). The electron ionized around 868.5 a.u. (G'_3) recombines with one of the protons and emits about the 50th harmonic around 1040 a.u. (G_3) corresponding to the suppressed harmonic emission G_3 shown in Fig. 4(a). In the U case, there are also three instants at which $\alpha = 0$, and they are marked in the Fig. 4(c) as U'_1, U'_2, and U'_3, respectively. The corresponding recombination times are also marked as U_1, U_2, and U_3 in the Fig. 4(a) and Fig. 4(c), respectively. The electron ionized from $\mathrm{H}(+)$ or $\mathrm{H}(-)$ around 900 a.u. recombines with one of the protons and emits the 60th harmonics around 972 a.u. which is in accordance with the suppressed harmonic emission U_1 shown in Fig. 4(b). At the instants of U_2 and U_3, the suppressed harmonic emissions are manifest in the time-frequency map [cf., Fig. 4(b)], but they are not obviously

linked to the spectrum minima due to the weaker intensity of the corresponding quantum paths. Therefore the suppressed harmonic emission is related to the moment of the counter-intuitive motion of electron and the mechanism of the HHG minimum is the consequence of the interference between the two phase-adiabatic states at the ionization time.

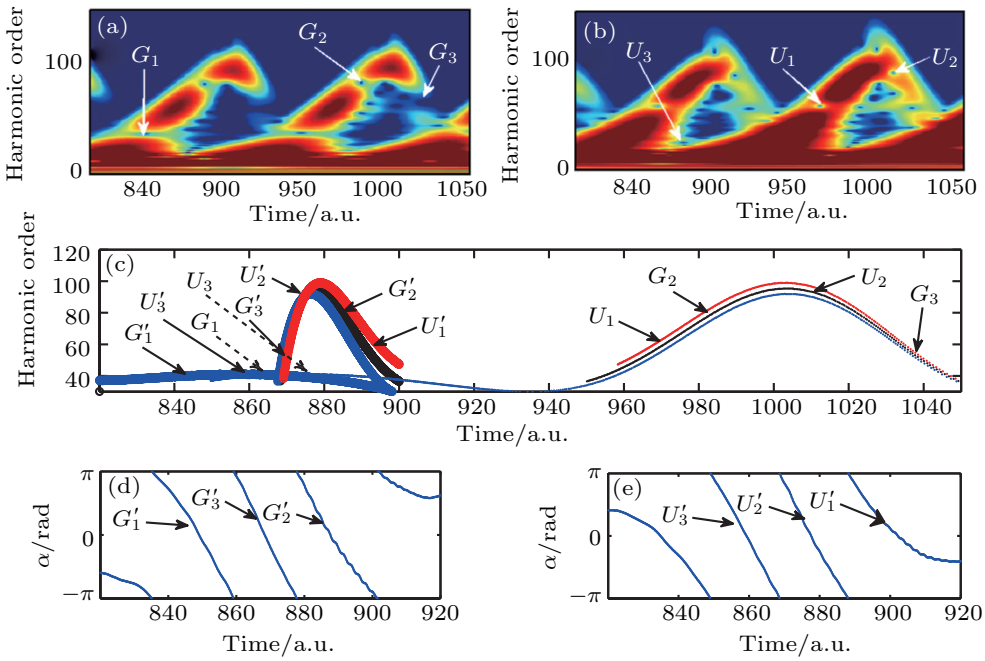


Fig. 4. (color online) ((a) and (b)) Time-frequency distributions of the electron dipole acceleration throughout recombination spanning 820 a.u.–1050 a.u. in the G case and in the U case, respectively. (c) Dependence of harmonic order on ionization time (circles) and emission time (dots) of the electron in the multicycle laser field. The laser parameters are the same as those in Fig. 2. ((d) and (e)) Evolving relative phase differences in the corresponding ionization time for the G case and the U case, respectively.

4. Conclusions

In this study, we demonstrate a new method to investigate the origin of spectral minimum in HHG. We calculate the HHG spectra generated from the 1D stretched H_2^+ interacting with multicycle midinfrared laser pulse initially in the ground state (G case) and the first excited state (U case), respectively. By varying the electronic state of the molecule, we find that the modulations of HHG, especially the positions of the minima change. According to the two-state model, we attribute the minima in the HHG spectra of stretched H_2^+ to the interference between the two phase-adiabatic states at the time of ionization. The difference between the minimum positions in the G case and U case is attributed to the different time-dependent interference which can lead to ultrafast interwell electron transfer. The result provides a new route to investigating the electronic structure and tracing the electronic dynamics in molecules by using the high-harmonic spectroscopy.

Acknowledgment

We sincerely thank Prof. Keli Han and Dr. Ruifeng Lu for providing us with the LZH-DICP code.

References

[1] Itatani J, Levesque J, Zeidler D, Niikura Hiromichi, Pépin H, Kieffer J C, Corkum P B and Villeneuve D M 2004 *Nature* **432** 867
[2] Le V H, Le A T, Xie R H and Lin C D 2007 *Phys. Rev. A* **76** 013414
[3] Vozzi C, Negro M, Calegari F, Sansone G, Nisoli M, De Silvestri S and Stagira S 2011 *Nat. Phys.* **7** 822
[4] Smirnova O, Mairesse Y, Patchkovskii S, Dudovich N, Villeneuve D, Corkum P and Ivanov M Y 2009 *Nature* **460** 972
[5] Shafir D, Soifer H, Bruner B D, Dagan M, Mairesse Y, Patchkovskii S, Ivanov M Y, Smirnova O and Dudovich N 2012 *Nature* **485** 343
[6] Xia C L and Miao X Y 2016 *J. At. Mol. Sci.* **7** 17
[7] Corkum P B 1993 *Phys. Rev. Lett.* **71** 1994
[8] Takemoto N and Becker A 2010 *Phys. Rev. Lett.* **105** 203004
[9] Takemoto N and Becker A 2011 *J. Chem. Phys.* **134** 074309
[10] Miller M R, Xia Y, Becker A and Jaroń-Becker A 2016 *Optica* **3** 259
[11] Miller M R, Jaroń-Becker A and Becker A 2016 *Mol. Phys.* (published online Dec. 27)
[12] Takemoto N and Becker A 2011 *Phys. Rev. A* **84** 023401
[13] Miao X Y and Zhang C P 2014 *Phys. Rev. A* **89** 033410
[14] Miller M R, Jaron-Becker A and Becker A 2016 *Phys. Rev. A* **93** 013406
[15] Kling M F, Siedschlag Ch, Verhoef A J, Khan J I, Schultze M, Uphues Th, Ni Y, Uiberacker M, Drescher M, Krausz F and Vrakking M J J 2006 *Science* **312** 246
[16] Kremer M, Fischer B, Feuerstein B, Jesus Vitor L B de, Sharma V, Hofrichter C, Rudenko A, Thumm U, Schr?ter C D, Moshammer R and Ullrich J 2009 *Phys. Rev. Lett.* **103** 213003
[17] Znakovskaya I, von den Hoff P, Marcus G, Zherebtsov S, Bergues B, Gu X, Deng Y, Vrakking M J J, Kienberger R, Krausz F, Vivie-Riedle R de and Kling M F 2012 *Phys. Rev. Lett.* **108** 063002
[18] Singh K P, He F, Ranitovic P, Cao W, De S, Ray D, Chen S, Thumm U, Becker A, Murnane M M, Kapteyn H C, Litvinyuk I V and Cocke C L 2010 *Phys. Rev. Lett.* **104** 023001
[19] Li L Q, Xu Y Y and Miao X Y 2016 *J. At. Mol. Sci.* **7** 1
[20] Kamta G L and Bandrauk A D 2005 *Phys. Rev. A* **71** 053407
[21] Kanai T, Minemoto S and Sakai H 2005 *Nature* **435** 470
[22] Vozzi C, Calegari F, Benedetti E, Caumes J P, Sansone G, Stagira S, Nisoli M, Torres R, Heesel E, Kajumba N, Marangos J P, Altucci C and Velotta R 2005 *Phys. Rev. Lett.* **95** 153902

[23] Le A T, Tong X M and Lin C D 2006 *Phys. Rev. A* **73** 041402
[24] Chen Y J and Liu J 2008 *Phys. Rev. A* **77** 013410
[25] Kanai T, Minemoto S and Sakai H 2007 *Phys. Rev. Lett.* **98** 053002
[26] Zhou X, Lock R, Li W, Wagner N, Murnane M M and Kapteyn H C 2008 *Phys. Rev. Lett.* **100** 073902
[27] Ciappina M F, Chirilă C C and Lein M 2007 *Phys. Rev. A* **75** 043405
[28] Baker S, Robinson J S, Lein M, Chirilă C C, Torres R, Bandulet H C, Comtois D, Kieffer J C, Villeneuve D M, Tisch J W G and Marangos J P 2008 *Phys. Rev. Lett.* **101** 053901
[29] Telnov D A and Chu S I 2007 *Phys. Rev. A* **76** 043412
[30] Wörner H J, Bertrand J B, Hockett P, Corkum P B and Villeneuve D M 2010 *Phys. Rev. Lett.* **104** 233904
[31] Lein M, Hay N, Velotta R, Marangos J P and Knight P L 2002 *Phys. Rev. Lett.* **88** 183903
[32] Li W, Zhou X B, Lock R, Patchkovskii S, Stolow A, Kapteyn H C and Murnane M M 2008 *Science* **322** 1207
[33] McFarland B K, Farrell J P, Bucksbaum P H and Gühr M 2008 *Science* **322** 1232
[34] He H X, Lu R F, Zhang P Y, Guo Y H, Han K L and He G Z 2011 *Phys. Rev. A* **84** 033418
[35] Chao Y, He H X, Wang Y H, Shi Q, Zhang Y D and Lu R F 2014 *J. Phys. B: At. Mol. Opt. Phys.* **47** 055601
[36] Seideman T, Ivanov M Y and Corkum P B 1995 *Phys. Rev. Lett.* **75** 2819
[37] Hu J, Han K L and He G Z 2005 *Phys. Rev. Lett.* **95** 123001
[38] Miao X Y and Du H N 2013 *Phys. Rev. A* **87** 053403
[39] Mulliken R S 1939 *J. Chem. Phys.* **7** 20
[40] Kulander K C, Mies F H and Schafer K J 1996 *Phys. Rev. A* **53** 2562
[41] Kawata I, Kono H and FujimuraY 1999 *J. Chem. Phys.* **110** 11152
[42] He F, Becker A and Thumm U 2008 *Phys. Rev. Lett.* **101** 213002